

DETC2002/MECH-34355

METRIC BASED DYNAMIC PARAMETER IDENTIFICATION FOR MOBILE FIELD MANIPULATOR SYSTEMS

Vivek A. Sujan

Department of Mechanical Engineering
Massachusetts Institute of Technology
Cambridge, MA 02139

Steven Dubowsky

Department of Mechanical Engineering
Massachusetts Institute of Technology
Cambridge, MA 02139

ABSTRACT

High performance robot control algorithms often rely on system physical models. For field robots, the dynamic parameters of these physical models may not be well known. This paper presents a new information based performance metric for the on-line dynamic parameter identification of a multi-body system. The metric is used in an algorithm to optimally regulate the external excitation required by the dynamic system identification proceeding. This algorithm is applied to identify the vehicle and suspension parameters of a mobile field manipulator. Issues addressed include the development of appropriate vehicle models (compatible with the onboard sensors), Kalman observer estimation of optimal parameter values, mutual information based observability (or identification) metric, and formulation of the manipulator exciting trajectory. Simulations and experimental results show the effectiveness of this algorithm.

1. INTRODUCTION

Future mobile field robotic systems, such as for planetary and terrestrial missions, will be required to perform complex tasks [Huntsberger, Shaffer]. In planetary exploration robots will be used to collect rock samples, to build infrastructures, explore complex terrains. Terrestrial tasks might include explosive ordinance removal, de-mining and handling hazardous waste, environment restoration [Baumgartner, Huntsberger, Osborn, Shaffer]. A field robot might be equipped with a manipulator arm and such onboard sensors such as inclinometers, accelerometers, vision systems, and force/torque sensors (see Figure 1). Control algorithms for such systems have been proposed that rely on accurate physical models of the system and its tasks [Hootsman]. To successfully apply such algorithms, accurate estimates of the dynamic parameters of the system are required. Although, these parameters may be ideally known from design data or found off-line by simple laboratory tests, for field systems in hostile environments, handling unknown payloads, they may not be well known in advance. For example, temperature fluctuations result in substantial changes in vehicle suspension stiffness and damping with time.

Vehicle fuel consumption, rock sample collection, etc. cause changes in the location of the center of gravity, the mass and the inertia of the system. Hence, on-line identification of these parameters can be critical for the system performance. This is a classical on-line identification problem: finding values of the parameters in the mathematical model of a system from on-line measured data such that the predicted dynamic response coincides with that of the real system.

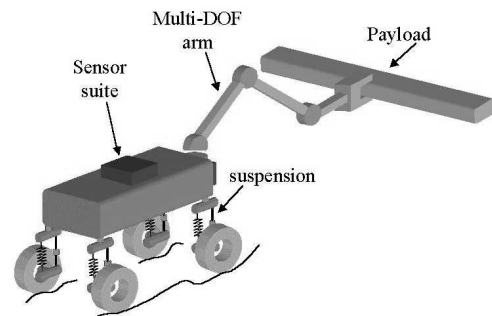


Figure 1: Representation of a general mobile field robot

Identification of system parameters is a well-studied problem [Alloum, Atkeson, Bard, Ljung, Nikravesh, Olsen, Serban, Schmidt, Soderstorm]. Various effective algebraic and numerical solution techniques have been developed to solve for unknown parameters using dynamic system models [Bard, Gelb, Nikravesh, Serban]. These include techniques based on pseudo-inverses, Kalman observers, Levenberg-Marquardt methods, and others. However, the accuracy/quality of the identified system parameters is a function of both the excitation imposed on the system as well as the measurement noise (sensor noise). A number of researchers have developed metrics to evaluate the quality of the identified system parameters [Armstrong, Gautier, Schmidt, Serban, Soderstorm]. Such metrics determine if a given set of parameters is identifiable, which is known as the “identifiability/observability” problem [Serban]. These include tests based on differential algebra, where a set of differential polynomials describes the model under consideration [Bard, Ljung]. Other metrics monitor the condition number of an excitation matrix computed from the

dynamic model. Examples of such excitation matrices include the Hessian of the model residual vector, the derivative of the system Hamiltonian, and the input correlation matrix [Serban, Gautier, Armstrong]. The metrics of parameter quality can be used to select the excitation imposed on the physical system and have been applied with limited success to industrial robotic systems [Armstrong, Atkeson, Gautier, Mayeda].

However, such approaches can be computationally complex, an important issue for space robots where computational power is very limited. For example, defining excitation trajectories for the identification of an industrial 3 DOF manipulator using an input correlation matrix requires 40 hours of VAX time [Armstrong, Gautier]. Additionally, these methods are unable to indicate which parameter estimates have low confidence values (low quality), since the quality metrics combines the performance into a single parameter. Thus it is not possible to assign higher weight to parameters of greater dynamic significance to system response.

In this paper, a new performance metric, called a mutual information based metric, is presented for the on-line dynamic parameter identification of a multi-body system. This metric measures on the uncertainty of each parameter's estimate. This measure is termed here the "parameter observability". The metric is used to formulate a cost function that optimally controls the external excitation to effectively identify the system dynamic parameters. The cost function weighs each parameter estimate according to its uncertainty. Hence, the excitation is controlled so that the identification favors parameters that have the greatest uncertainty at any given time. This method is computationally more efficient and yields faster convergence than single parameter methods. Also parameters may be given greater importance in the cost function based on its significance to the system's dynamic response.

Here the algorithm is applied to the on-line parameter identification of a mobile field robot system and is shown to be computationally efficient. An onboard manipulator arm (with bandwidth constraints) is moved to generate reaction forces, which excite vehicle base motions. The dynamic parameters include the mass, location of center of gravity, the inertia, base compliance and damping. The method assumes a robotic system composed of rigid elements, and no relative motion of vehicle wheels to ground during the identification process. The algorithm also assumes that robot is equipped with an inclinometer, an accelerometer and an arm base force/torque sensor. It is assumed that the onboard manipulator dynamic parameters are known and the bandwidth of the arm actuators is sufficiently high, to excite the vehicle dynamics. Finally, small motions of base compliance are assumed to occur. The system is modeled using a Newton-Euler formulation. A Kalman filter is used to solve the dynamic parameters based on the physical model. The mutual information based observability metric is used to determine the arm excitation trajectory. Simulation and experimental results show the effectiveness of this algorithm.

2. SYSTEM DYNAMIC MODEL

The algorithm to generate arm excitation trajectories for parameter identification, requires a dynamic model of the system. A number of models of vehicle suspension systems have been proposed [Alloum, Halfmann, Harris, Majjad,

Nelles]. Many of these are quarter or half-vehicle models that consider stiffness and damping coefficients, but neglect vehicle mass and inertial properties. Here, a Newton-Euler formulation is used to provide the full spatial dynamics of the system. The system represented in Figure 1, is reduced to three components: a rigid arm, a rigid vehicle body and a compliance module (see Figure 2). These three components interact dynamically. Rotational motions of the rigid arm about an axis in frame IV (Figure 3a) result in reaction forces/moments felt by the vehicle base (Figure 3b) and in the suspension module (Figure 4). Motions of the base are measured through the onboard inclinometer and accelerometer. Interaction forces/torques between the arm and the vehicle base are measured by a base force/torque sensor (origin coincides with frame VI—Figure 2).

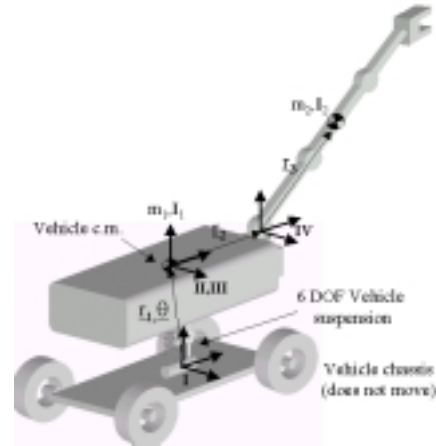


Figure 2: Representation of the simplified mobile robot

Although, the real vehicle has a complex, multi-element suspension system, only the net base compliance is modeled. This is modeled as a 6 DOF linear stiffness and damping system, located at the vehicle base center-of-gravity. For small base motions, this bulk model of the suspension is sufficient to accurately model the vehicle dynamics. An advantage of the bulk suspension, is that all coefficients can be identified by only observing the vehicle base motions, thus eliminating the need for the placement of more exotic sensors at each individual suspension. Additionally, a bulk suspension model accounts for all sources of compliance that would be difficult to model and measure individually.

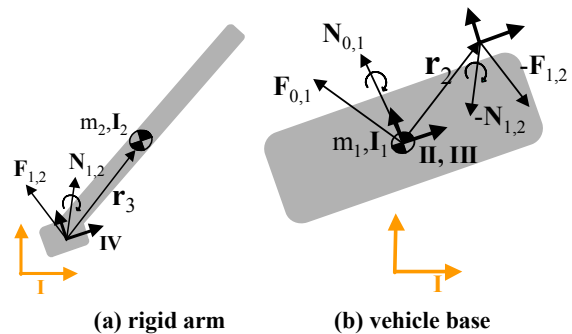


Figure 3: Force/moment balance

The spatial interaction forces/moments of the rigid arm are:

$$\begin{aligned}
 (\mathbf{F}_{1,2})_{IV} + (m_2 \mathbf{g})_{IV} &= (m_2 \mathbf{a}_{cm_2})_{IV} \\
 (\mathbf{N}_{1,2})_{IV} - (\mathbf{r}_3 \times \mathbf{F}_{1,2})_{IV} &= \left(\frac{\partial (\mathbf{I}_2^{cm} \boldsymbol{\omega}_2^{cm})}{\partial t} + \boldsymbol{\omega}_2^{cm} \times (\mathbf{I}_2^{cm} \boldsymbol{\omega}_2^{cm}) \right)_{IV} \quad (1) \\
 (\mathbf{F}_{1,2})_{IV} \text{ and } (\mathbf{N}_{1,2})_{IV} &\Rightarrow \text{from arm base F/T sensor}
 \end{aligned}$$

where \mathbf{F}_{12} and \mathbf{N}_{12} are the reaction forces and moments, m_2 and \mathbf{I}_2 are the arm mass and inertia tensors, \mathbf{a}_2 and $\boldsymbol{\omega}_2$ are the arm linear acceleration and angular velocity vectors. The spatial interaction forces/moments of the rigid base are:

$$\begin{aligned} (\mathbf{F}_{0,1})_{II} &= (m_1 \mathbf{a}_{cm_1})_{II} - (-\mathbf{F}_{1,2})_{II} - (m_1 \mathbf{g})_{II} \\ (\mathbf{N}_{0,1})_{II} &= \left(\frac{\partial (\mathbf{I}_1^{cm} \boldsymbol{\omega}_1^{cm})}{\partial t} + \boldsymbol{\omega}_1^{cm} \times (\mathbf{I}_1^{cm} \boldsymbol{\omega}_1^{cm}) \right)_{II} - (-\mathbf{N}_{1,2})_{II} + (\mathbf{r}_2 \times \mathbf{F}_{1,2})_{II} \end{aligned} \quad (2)$$

where \mathbf{F}_{01} and \mathbf{N}_{01} are the reaction forces and moments, m_1 and \mathbf{I}_1 are the base mass and inertia tensors, \mathbf{a}_1 and $\boldsymbol{\omega}_1$ are the base linear acceleration and angular velocity vectors.

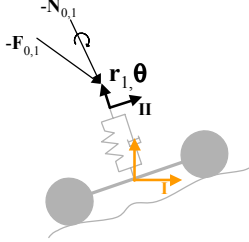


Figure 4: Force/moment balance of compliance module

Finally, the spatial interaction forces/moments of the compliance module are given by:

$$\begin{aligned} d(-\mathbf{F}_{0,1})_{II} &= \mathbf{b}_r^T \cdot d\dot{\mathbf{r}}_1 + \mathbf{k}_r^T \cdot d(\mathbf{r}_1 - \mathbf{r}_1^0) \\ d(-\mathbf{N}_{0,1})_{II} &= \mathbf{b}_\theta^T \cdot d\dot{\boldsymbol{\theta}} + \mathbf{k}_\theta^T \cdot d(\boldsymbol{\theta} - \boldsymbol{\theta}^0) \end{aligned} \quad (3)$$

where \mathbf{k}_r and \mathbf{k}_θ are the translational and rotational stiffness coefficients, \mathbf{b}_r and \mathbf{b}_θ are the translational and rotational damping coefficients. Using Equations 1, 2 and 3 a set of 6 dynamic equations is obtained (forces and moments in 3D):

$$\begin{aligned} m_1 (d(\mathbf{R}_0^T \mathbf{g}) - d(\ddot{\mathbf{r}}_1)_{II}) - \mathbf{b}_r^T \cdot d\dot{\mathbf{r}}_1 - \mathbf{k}_r^T \cdot d\mathbf{r}_1 &= d(\mathbf{F}_{1,2})_{II} \\ -\mathbf{I}_1 d(\ddot{\boldsymbol{\theta}})_{II} - d(\dot{\boldsymbol{\theta}} \times (\mathbf{I}_1 \dot{\boldsymbol{\theta}}))_{II} - d(\mathbf{r}_2 \times \mathbf{F}_{1,2})_{II} - \mathbf{b}_\theta^T \cdot d\dot{\boldsymbol{\theta}} - \mathbf{k}_\theta^T \cdot d\boldsymbol{\theta} &= d(\mathbf{N}_{1,2})_{II} \end{aligned} \quad (4)$$

Using the onboard sensors described above, this set of equations present the following unknowns, knowns, and measurable quantities:

unknowns: $m_1, \mathbf{I}_1, \mathbf{r}_2, \mathbf{k}_r, \mathbf{b}_r, \mathbf{k}_\theta, \mathbf{b}_\theta$

knowns: m_2, \mathbf{I}_2

measured: $d\mathbf{r}_1, d\dot{\mathbf{r}}_1, d\ddot{\mathbf{r}}_1$ (III w.r.t. II), $d\boldsymbol{\theta}, d\dot{\boldsymbol{\theta}}, d\ddot{\boldsymbol{\theta}}$ (II w.r.t. I)

It is important to observe that only the changes in linear/angular position of the base can be measured. The 6 dynamic equations of motion are evaluated for three rotation modes or the arm (rotation about the x, y and z axes) giving a total of 18 independent equations. Note that the arm rotation occurs only about the base joints. The remaining joints are held fixed. This configuration is sufficient to produce the dynamic forces required to generate the needed vehicle excitations. Additionally, this maintains the generality of the algorithm developed in this paper, as no specific manipulator kinematics are assumed (other than two base rotational joints).

3. ESTIMATING THE DYNAMIC PARAMETERS

Two common solution methods used for equations of the form $\mathbf{A} \mathbf{x} = \mathbf{F}$ (where \mathbf{A} is a known matrix, \mathbf{x} is a vector of unknowns, and \mathbf{F} is a known vector) are pseudo-inverse and Kalman filters. Both result in a least-squares solution to the problem. Note that equation 4 is easily cast into this form.

In a pseudo-inverse solution process, a discrete set of measurements combined with the 18 equations are used to formulate the matrix \mathbf{A} and the vector \mathbf{F} . A solution to $\mathbf{A} \mathbf{x} = \mathbf{F}$

is simply given by: $\mathbf{x} = (\mathbf{A}^T \mathbf{A})^{-1} \mathbf{A}^T \mathbf{F}$.

A more efficient solution is to use a Kalman filter [Gelb]. A Kalman filter is a multiple-input, multiple-output digital filter that can optimally estimate, in real time, the states of a system based on its noisy outputs. These states are all the variables needed to completely describe the system behavior as a function of time. The measurements are statistically optimum in the sense that they minimize the mean-square estimation error. Here, rather than estimating \mathbf{x} based on one large matrix \mathbf{A} (containing all the measurements), \mathbf{x} is estimated based on a single set of measurements and an associated covariance matrix is developed. With each new measurement set, the estimate is improved and the covariance updated. Since, there are numerous articles in the literature describing Kalman filters, only a flow-diagram of the process is presented here (see Figure 5). In Figure 5, \mathbf{Q}_k models the uncertainty which corrupts the system model, \mathbf{R}_k models the uncertainty associated with the measurement and \mathbf{C}_k gives total uncertainty of the state estimate [Bard, Gelb, Nikravesh].

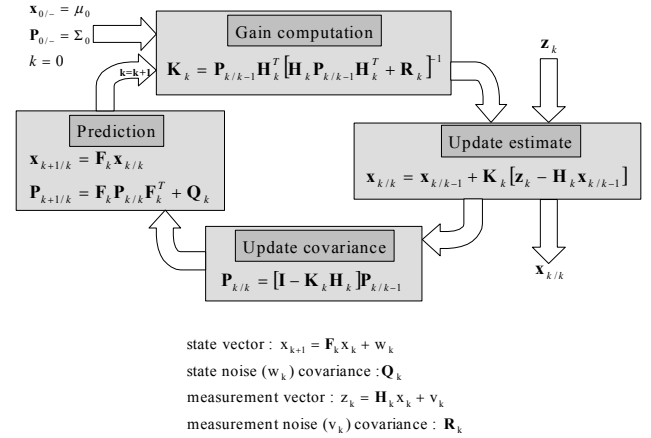


Figure 5: Flow-diagram of a Kalman Filter

4. A METRIC FOR OBSERVABILITY

Although, the above methods (pseudo-inverse and Kalman filter) produce solutions to the unknown dynamic parameters, a fundamental issue on the observability of unknown parameters is still to be addressed. Essentially, this provides a measure of accuracy of the current solution for a dynamic parameter. This is a difficult issue and a-priori tests are not available.

4.1. Classical observability metric

Classically, the concept of observability in the control literature is defined from a state model of the dynamic system. The idea is to determine if there are a sufficient number of independent equations that relate the system states, and from which these states may be inferred. Formally, a system is observable if the initial state can be determined by observing the output for some finite period of time. This metric is briefly outlined here and a discrete formulation is presented.

The linear system model (or state model) for a typical process (in the absence of a forcing function) is given by:

$$\dot{\bar{\mathbf{x}}} = \mathbf{F}\bar{\mathbf{x}} + \mathbf{G}\bar{\mathbf{w}} \quad \text{state model} \quad (5)$$

$$\bar{\mathbf{z}} = \mathbf{H}\bar{\mathbf{x}} + \bar{\mathbf{v}} \quad \text{observation model}$$

The discrete model is implemented by converting the continuous time model, given by:

$$\bar{\mathbf{x}}_{k+1} = \Phi_k \bar{\mathbf{x}}_k + \Gamma_k \bar{\mathbf{w}}_k \quad \text{state model} \quad (6)$$

$$\bar{\mathbf{z}}_k = \mathbf{H}_k \bar{\mathbf{x}}_k + \bar{\mathbf{v}}_k \quad \text{observation model}$$

where

\bar{x}_k is the (n x 1) system state vector at time t_k

Φ_k is the (n x n) transition matrix which relates \bar{x}_k to \bar{x}_{k+1}

Γ_k is the (n x n) process noise distribution matrix

\bar{w}_k is an (n x 1) white disturbance sequence with known covariance structure

\bar{z}_k is an (m x 1) measurement at time t_k

H_k is an (m x n) measurement matrix or observation matrix

\bar{v}_k is an (m x 1) white measurement noise sequence with known covariance

When the F matrix is constant in time and the equation is linear, then the transition matrix is a function only of the time step dt, and is given by the matrix exponential:

$$\Phi_k = e^{F\Delta t} = I + F\Delta t + \frac{(F\Delta t)^2}{2!} + \dots \quad (7)$$

It is assumed that process and measurement noise sequences are uncorrelated in time (white) and uncorrelated with each other. In practice, the transition matrix can often be written by inspection. When dt is much smaller than the dominant time constants in the system, just a two term approximation is sufficient. Consider the discrete nth order constant coefficient linear system, $\bar{x}_{k+1} = \Phi_k \bar{x}_k$, for which there are m noise free measurements, $z_k = Hx_k$ (where $k=0\dots m-1$), where each H is an (m x n) matrix. The sequence of the first i measurements can be written as:

$$\begin{aligned} z_0 &= Hx_0 \\ z_1 &= Hx_1 = H\Phi x_0 \\ z_2 &= Hx_2 = H\Phi^2 x_0 \\ &\vdots \\ z_{i-1} &= Hx_{i-1} = H\Phi^{i-1} x_0 \end{aligned} \quad (8)$$

This can be written as the augmented set of equations, $Z = \Xi^T x_0$. If the initial state is to be determined from this sequence of measurements then $\Xi = [H^T | \Phi^T H^T | \dots | (\Phi^T)^{n-1} H^T]$

must have rank n. This definition is limited in that it does not account for the effects of corrupted (noise) data. Additionally, the unobservable state cannot be determined. To address both problems, a new mutual information based metric is proposed below.

4.2. Mutual information based metric

Suppose a set of possible events with known probabilities of occurrence of p_1, p_2, \dots, p_n exists. If there is a measure of the amount of "choice" is involved in selecting an event, $H(p_1, p_2, \dots, p_n)$, it is reasonable to require of it the following properties [Shannon]:

1. H should be continuous in the p_i .
2. If all the p_i are equal, $p_i=1/n$, then H should be a monotonic increasing function of n.
3. If a choice be broken down into two successive choices, the original H should be the weighted sum of the individual values of H.

It has been shown that the only H satisfying the three assumptions is of the form (where K is a positive constant)

[Shannon]:

$$H = -K \sum_{i=1}^n p_i \log p_i \quad (9)$$

Now consider the case where the signal is perturbed by noise during transmission i.e. the received signal is not necessarily the same as that sent out by the transmitter. Two cases may be distinguished. If a particular transmitted signal always produces the same received signal, i.e. the received signal is a definite function of the transmitted signal, then the effect is called distortion. If this function has an inverse—no two transmitted signals produce the same received signal—distortion may be corrected. The case of interest here is when the signal does not always undergo the same change in transmission. In this case the received signal, Y, is a function of the transmitted signal, X, and a second variable, the noise N: $Y=f(X,N)$. The noise is considered to be a chance variable. In general it may be represented by a suitable stochastic process. A finite number of states and a set of probabilities is assumed: $p_{\alpha,i}(\beta,j)$. This is the probability, if the channel is in state α and the symbol i is transmitted, that the symbol j will be received and the channel left in state β . Thus α and β range over the possible states, i over the possible transmitted signals and j over the possible received signals. In the case where successive symbols are independently perturbed by the noise there is only one state, and the channel is described by the set of transitional probabilities $p_i(j)$, the probability of transmitted symbol i being received as j [Shannon].

Thus, if a noisy channel is fed by a source there are two statistical processes at work: the source and the noise. A number of important entropies can be calculated: the entropy of the source, $H(x)$; the entropy of the output of the channel, $H(y)$; the joint entropy of input and output, $H(x,y)$; the conditional entropies $H(y|x)$ and $H(x|y)$, the entropy of the output when the input is known and conversely. In the noiseless case $H(y)=H(x)$. All these can be measured on a per-second or per-symbol basis. For a discrete channel transmitting a signal, an analogy with a sensor is made. The signal being read is the true value of the parameter being measured. The signal transmitted is the value that the sensor provides to a computer of the measured value (corrupted by noise).

The above definitions are used to get a handle on the amount of information being transmitted by such a sensor i.e. the measure for observability. Consider the random variables x and y with joint probability distribution $p(x_i, y_j)$, $1 \leq i \leq N$, $1 \leq j \leq M$. The conditional entropy of x given y is defined as:

$$H(x|y) = - \sum_{i=1}^N \sum_{j=1}^M p(x_i, y_j) \log_2 p(x_i | y_j) \quad (10)$$

$H(x|y)$ can be interpreted as the average amount of uncertainty about x after y has been revealed. Some important properties of the conditional entropy can be derived [Shannon]:

- (i) $H(x|y) \leq H(x)$ with equality iff x and y are independent.
- (ii) $H(x,y) = H(y) + H(x|y) = H(x) + H(y|x)$

The average amount of information about x contained in y can now be defined in terms of the reduction in the uncertainty of x upon disclosure of y. Denoting this information by $I(x,y)$, define:

$$I(x,y) = H(x) - H(x|y) \quad (11)$$

With the aid of property (ii), it is easy to show that:

$$I(y,x) = H(y) - H(y|x) = I(x,y) \quad (12)$$

Thus, the information about x contained in y is equal to the information about y contained in x . For this reason, $I(x,y)$ is called the average mutual information between x and y . From property (i), $I(x,y) \geq 0$ with equality iff x and y are independent. As a direct consequence of the definition of $I(x,y)$:

$$I(\mathbf{x}, \mathbf{y}) = \sum_{i=1}^N \sum_{j=1}^M p(x_i, y_j) \log_2 \frac{p(x_i, y_j)}{p(x_i)p(y_j)} \quad (13)$$

Sensor noise is now modeled. A single observation of a point (\bar{x}) is modeled as a Gaussian probability distribution centered at \bar{x} . The selection of a Gaussian function to model uncertainty in sensor data is based on two important observations. The use of the mean and the covariance of a probability distribution function is a reasonable form to model sensor data and is a second order linear approximation. This linear approximation corresponds to the use of a Gaussian (having all higher moments of zero). Additionally, based on the central limit theorem, the sum of a number of independent variables has a Gaussian distribution regardless of their individual distributions. The canonical form of the Gaussian distribution in 3 dimensions depends on the standard distributions, $\sigma_{x,y,z}$, a covariance matrix (C) and the mean (\bar{x}) [Ljung, Nikravesh]:

$$p(\bar{x}' | \bar{y}) = \frac{1}{(2\pi)^{3/2} \sqrt{|C|}} \exp\left(-\frac{1}{2}(\bar{y} - \bar{x}')^T C^{-1}(\bar{y} - \bar{x}')\right) \quad (14)$$

$$\text{where } C = \begin{bmatrix} \sigma_x^2 & \rho\sigma_x\sigma_y & \rho\sigma_x\sigma_z \\ \rho\sigma_x\sigma_y & \sigma_y^2 & \rho\sigma_y\sigma_z \\ \rho\sigma_x\sigma_z & \rho\sigma_y\sigma_z & \sigma_z^2 \end{bmatrix}$$

where the exponent is called the Mahalanobis distance. For uncorrelated measured data $\rho=0$. This can be generalized for an n dimensional sensor. $H(x)$ and $H(x|y)$ can be explicitly defined in terms of a given sensor:

$$H(x) = \sum_{i=1}^n p_i \log p_i \quad \text{where } p_i = \frac{1}{n}$$

and n = number of sensor discrete states

$$H(x|y) = \sum_{i=0}^{n-1} q_i \log q_i \quad \text{where } q_i = \frac{\int_a^b p(\bar{x}' | \bar{y}) d\bar{x}'}{\int_{\min}^{\max} p(\bar{x}' | \bar{y}) d\bar{x}'}$$

$$\text{and } \begin{cases} a = \min + i \left(\frac{\max - \min}{n} \right); b = \min + (i+1) \left(\frac{\max - \min}{n} \right) \\ \max = \text{maximum sensor reading;} \\ \min = \text{minimum sensor reading} \\ p(\bar{x}' | \bar{y}) \text{ is obtained from Equation 14} \end{cases} \quad (15)$$

Thus, $I(y,x)$, reflects the information content of the current estimate of the dynamic parameter being estimated. Although, this metric makes no assumption on the form of noise (Gaussian, etc.), it is convenient to establish the details using Gaussian noise.

5. FORMULATION OF EXCITING TRAJECTORIES

Using the observability metric defined in Section 4, a method to formulate the appropriate arm-exciting trajectory is

now developed. The basic idea is to use the estimation of the dynamic parameters, combined with the observability metric, to modify the arm motion. The goal is to increase the observability associated with the dynamic parameter estimates.

From Section 2 a set of differential algebraic equations of motion of the form: $\mathbf{Ax} = \mathbf{F}$ is obtained. In the situation considered here, the excitation function is sinusoidal, namely $f(t) = a_0 + a \sin(\omega t)$ (Equation 1). The only parameters that can be varied to change the excitation of the robotic base are the amplitude, frequency and offset of the sinusoidal excitation function i.e. amplitude (a), frequency (ω) and offset (a_0) of motion of the robotic arm.

Based on the associated information (Section 4) for the estimate, \tilde{x}_k , a cost function is defined as follows:

$$\begin{aligned} V(\mathbf{d}) &= \frac{1}{2} \sum_i \left(1 - \left(1 - \frac{I_{x_i}}{I_{x_i}^{\max}} \right) \frac{I_{x_i}}{I_{x_i}^{\max}} \right) \\ &= \frac{1}{2} \sum_i \left(1 - \frac{I_{x_i}}{I_{x_i}^{\max}} + \left(\frac{I_{x_i}}{I_{x_i}^{\max}} \right)^2 \right) = \frac{1}{2} \sum_i r_i^2(\mathbf{d}) \end{aligned} \quad (16)$$

where i is summed over the number of dynamic parameters to identify. $I_{x_i}^{\max}$ is the current maximum information (observability) associated with any of the parameter estimates. Note, in this cost function the information associated with each parameter is weighted such that parameters with a higher uncertainty receive a higher weight. Further, this cost function may be easily amended to include weightings that reflect the relative importance of the individual dynamic parameters. A numerical minimization routine is applied to this cost function, by changing the excitation function in amplitude, frequency and offset (the current estimates for the unknowns are used here). The control parameters vector $\mathbf{d} \in \mathbf{R}^3$ consists of the amplitude, frequency and offset of the arm excitation function. By assembling the terms $r_i(\mathbf{d})$ into a vector $\mathbf{R}(\mathbf{d})$, given as:

$$\mathbf{R}(\mathbf{d}) = \{r_1(\mathbf{d}), \dots, r_{n_m}(\mathbf{d})\}^T \quad (17)$$

the control parameters \mathbf{d} must be chosen so that the residual vector \mathbf{R} is as small as possible. The quadratic cost function $V(\mathbf{d})$ of Equation 16 becomes:

$$V(\mathbf{d}) = \frac{1}{2} \mathbf{R}^T(\mathbf{d}) \mathbf{R}(\mathbf{d}) \quad (18)$$

The problem of finding \mathbf{d} from $V(\mathbf{d})$ is a nonlinear least-squares problem [Nikravesh]. If the vector $\mathbf{R}(\mathbf{d})$, is continuous, and if both first and second-order derivatives are available, then the nonlinear least-squares problem can be solved by standard unconstrained optimization methods. Otherwise, a method that requires only the first derivatives of $\mathbf{R}(\mathbf{d})$ must be used [Serban]. The first derivative of Equation 18 with respect to the design parameters, \mathbf{d} , is defined as:

$$G(\mathbf{d}) = \sum_{i=1}^{n_m} \nabla r_i(\mathbf{d}) r_i(\mathbf{d}) = \mathbf{J}^T(\mathbf{d}) \mathbf{R}(\mathbf{d}) \quad (19)$$

where $\mathbf{J}(\mathbf{d}) \in \mathbf{R}^{n_m \times 3}$ is the Jacobian matrix of $\mathbf{R}(\mathbf{d})$ with respect to the design parameters. The second derivative of Equation 18 with respect to the design parameters, \mathbf{d} , is defined as:

$$H(\mathbf{d}) = \sum_{i=1}^{n_m} [\nabla r_i(\mathbf{d}) r_i(\mathbf{d})^T + \nabla^2 r_i(\mathbf{d}) r_i(\mathbf{d})] = \mathbf{J}^T(\mathbf{d}) \mathbf{J}(\mathbf{d}) + \mathbf{S}(\mathbf{d}) \quad (20)$$

where $\mathbf{S}(\mathbf{d}) \in R^{3 \times 3}$ is part of $\mathbf{H}(\mathbf{d})$ that is a function of second derivatives of $\mathbf{R}(\mathbf{d})$. Thus the knowledge of $\mathbf{J}(\mathbf{d})$ supplies $\mathbf{G}(\mathbf{d})$ and the part of $\mathbf{H}(\mathbf{d})$ dependent on first-order derivative information, but not on the second order part $\mathbf{S}(\mathbf{d})$. Levenberg-Marquardt methods simply omit $\mathbf{S}(\mathbf{d})$ and base the step selection (\mathbf{d}') on the approximation given by [Serban]:

$$V(\mathbf{d} + \mathbf{d}') = V(\mathbf{d}) + \mathbf{G}^T(\mathbf{d})\mathbf{d}' + \frac{1}{2}\mathbf{d}'^T \mathbf{J}^T(\mathbf{d})\mathbf{J}(\mathbf{d})\mathbf{d}' \quad (21)$$

Equation 21 leads to the following optimization procedure:

$$\mathbf{d}^{(k+1)} = \mathbf{d}^{(k)} + \alpha_k \mathbf{d}'^{(k)} \quad (22)$$

with

$$\mathbf{d}'^{(k)} = \frac{-\mathbf{G}(\mathbf{d}^{(k)})}{\mathbf{J}^T(\mathbf{d}^{(k)})\mathbf{J}(\mathbf{d}^{(k)})} \quad (23)$$

$$\alpha_k = \arg \min_{\alpha} [V(\mathbf{d}^{(k)} + \alpha \mathbf{d}'^{(k)})]$$

$\mathbf{d}'^{(k)}$ given by Equation 23 represents a descent direction. Thus, using equations 22 and 23, the amplitude, frequency and offset of the robot arm is refined during the identification process, leading to an optimal excitation trajectory. Note that in physical systems evaluation of the information metric and refining of the arm motion should be carried out at time intervals larger than the sampling time. This permits the physical system to respond sufficiently to the changes in arm motion.

6. RESULTS

6.1. Simulation

Two Tests have been conducted using a 3D simulation of a mobile robot system with a manipulator and suspension compliance. The first uses a constant parameter excitation function to drive the arm. The second uses a variable parameter excitation function (based on the formulation presented above) to drive the arm. The parameter identification results are compared. The system was simulated for 10 seconds. The manipulator arm mass is assumed to be 1Kg and inertia, $I_x=0.02\text{kg}\cdot\text{m}^2$ $I_y=0.001\text{kg}\cdot\text{m}^2$ $I_z=0.02\text{kg}\cdot\text{m}^2$ $I_{xz}=0$ $I_{yz}=0$ $I_{xy}=0$ $I_{yx}=0$ $I_{zy}=0$ $I_{zx}=0$ $I_{yz}=0$ $I_{xy}=0$ $I_{yx}=0$ $I_{zy}=0$ $I_{zx}=0$. In the simulation, sensor data is corrupted by adding white noise of upto 10% of the maximum sensed value. Evaluation of the information metric and refining arm motion occur ever 0.4 secs, with a sampling time of 0.005 secs.

For the first case, the constant parameter excitation function is given by the simple form:

$$f(t) = a_0 + a \cdot \sin(\omega t) = \pi/4 + 2\pi/9 \cdot \sin(\pi/2 t) \quad (24)$$

Figures 6 and 7 show the arm excitation functions for the two test cases. Figure 8 shows the value for the mutual information metric in identifying the stiffness in θ_p for the two test cases. Figure 9 shows the convergence in identification of the stiffness in θ_p for the two test cases. Table 1 presents the identification results of the 22 unknowns (see Section 2) using both arm excitation tests. The average percentage error shows an improvement of almost a factor of six for the variable parameter over the constant parameter excitation function. The average computational time per evaluation step for 22 unknown parameters with $I_{x_i}^{\max}=10$ bits on a PIII 750MHz platform is 75 ms. For comparison, the simulation is run using a parameter quality metric based on the condition number a matrix formed by the sensed values (matrix \mathbf{A} in section 3). On average, parameter estimates converge an order of magnitude faster (in simulation time) using the information based quality metric.

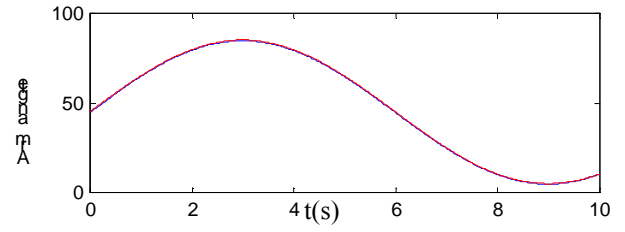


Figure 6: Constant parameter arm motion

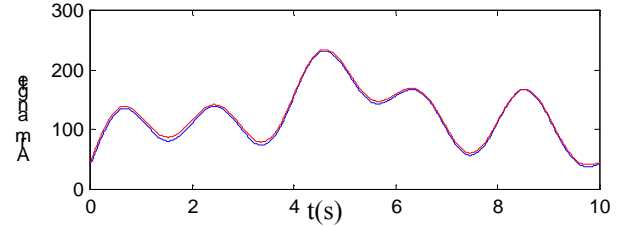
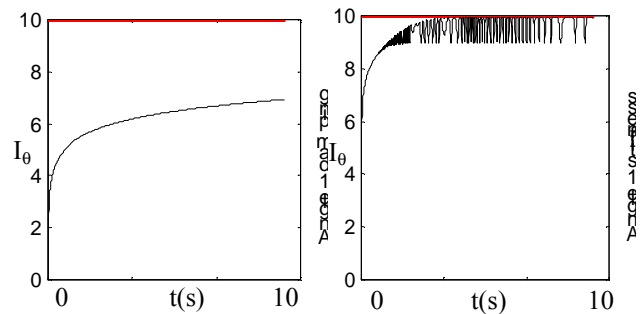


Figure 7: Variable parameter arm motion

Table 1: Simulation parameter identification

Parameter	True value	Constant parameter excitation function	Variable parameter excitation function
Mass (kg)	3.0	4.021	3.655
Inertia I_x (kg-m ²)	0.15	0.123	0.144
Inertia I_y (kg-m ²)	0.10	0.054	0.089
Inertia I_z (kg-m ²)	0.20	0.119	0.177
Inertia I_{yz} (kg-m ²)	0.0	0.045	0.011
Inertia I_{zy} (kg-m ²)	0.03	0.071	0.047
Inertia I_{xy} (kg-m ²)	0.0	0.037	0.014
c.g. x (m)	0.01	0.030	0.012
c.g. y (m)	0.3	0.512	0.360
c.g. z (m)	0.1	-1.053	0.042
Damping x (kg/s)	100	142.554	78.362
Damping y (kg/s)	100	139.956	75.559
Damping z (kg/s)	300	22.368	16.757
Damping θ_p (kg/s)	200	78.665	195.264
Damping θ_r (kg/s)	300	105.061	266.254
Damping θ_v (kg/s)	400	133.714	333.860
Stiffness x (kg/s ²)	1000	1103.281	979.494
Stiffness y (kg/s ²)	1000	1094.529	1244.836
Stiffness z (kg/s ²)	500	390.469	375.479
Stiffness θ_p (kg/s ²)	2000	945.103	1934.569
Stiffness θ_r (kg/s ²)	2500	1950.426	2394.257
Stiffness θ_v (kg/s ²)	3000	2402.537	2891.637
% Avg. Error		108.8	18.9



(a) constant parameter excitation function

(b) variable parameter excitation function

Figure 8: Mutual information metric for Stiffness θ_p

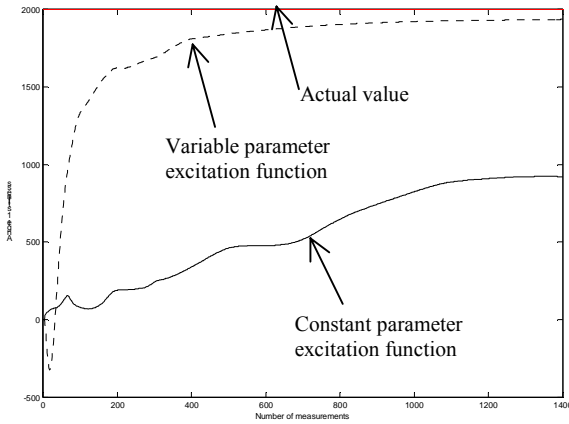


Figure 9: identification of Stiffness θ_p

6.2. Experiments

The experimental platform consists of a four-wheeled robot with a four DOF manipulator arm mounted on a 6-axis force/torque sensor (see Figure 10). On-board sensors also includes a two-axis inclinometer. An off-board computer system (Pentium 166 MHz) is used for real-time control, data acquisition, and data processing. All programs are written in C++ operating on Windows NT. Due to the absence of an accelerometer in the current experimental platform, tests only demonstrate the identification of rotational dynamic components (inertia, stiffness, damping of roll/pitch axes and the location of the center of gravity).

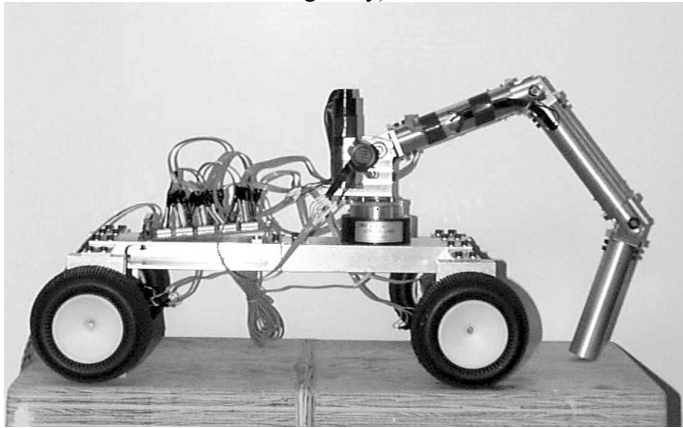


Figure 10: Experimental mobile manipulator

Before any parameters identification tests are run using the algorithm developed above, the real dynamic parameters must be identified. Conventional laboratory approaches are used here [Bard, Nikravesh, Serban]. Mass is measured using a precision weighing scale. The location of the center of mass is found by tilting the vehicle on one axis supported at two points, and measuring the reaction forces at the support points. Inertia is measured using pendulum oscillatory tests. Stiffness is measured by measuring deflection as a function of added load. Damping is measured by fitting the impulse response of the system to a second order equation. Linear models are used for stiffness and damping tests. Use of the force/torque sensor in the experimental system eliminates the need to measure the actual arm inertia tensor (see Equation 4).

Again, two main tests have been conducted using the constant parameter excitation function (similar in form as

before) and the variable parameter excitation function to drive the arm. The parameter identification results are compared. The experiments were run for approximately 10 seconds. Figures 11 and 12 show the arm excitation functions for the two test cases. Figure 13 shows the inclinometer pitch reading for the 2 test cases.

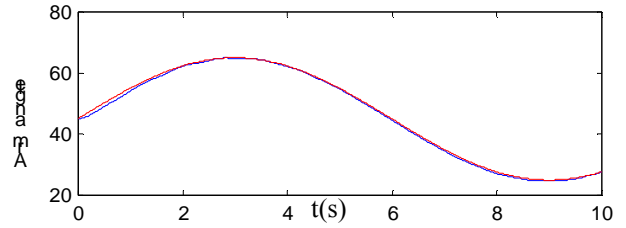


Figure 11: Constant parameter arm motion

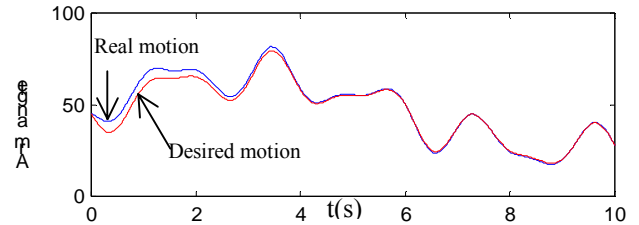


Figure 12: Variable parameter arm motion

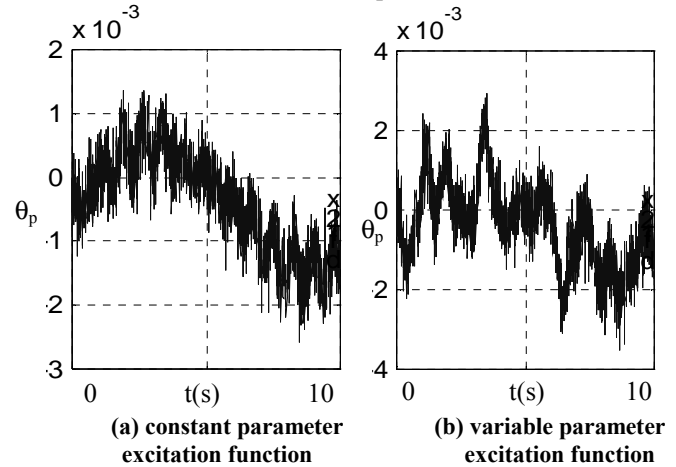


Figure 13: Inclinometer pitch reading (radians)

Table 2: Experimental parameter identification

Parameter	True value	Constant parameter excitation function	Variable parameter excitation function
Inertia x	0.072	0.041	0.035
c.g. y	0.054356	-0.072	0.072
c.g. z	0.036195	-0.091	0.052
Damping θ_p	1.5	7.543	1.459
Stiffness θ_p	317.0	354.711	327.885
% Avg. Error		208.4	26.8

Table 2 presents the identification results of the five unknowns using both arm excitation tests. The average percentage error shows an improvement of almost a factor of 8 for the variable parameter over the constant parameter excitation function. Figure 14 shows the convergence in identification of the

stiffness in θ_p for the two test cases. In addition to the significant corruption of data due to sensor noise, inaccuracies in laboratory measurements of “true” vehicle dynamic parameters contribute to the errors seen.

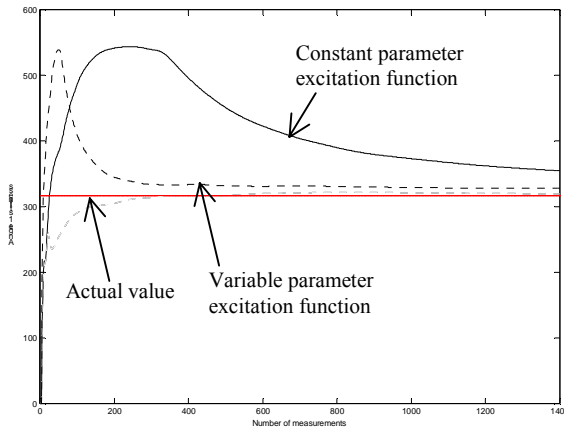


Figure 14: identification of Stiffness θ_p

7. CONCLUSIONS

This paper presents an algorithm based on iterative excitation of vehicle dynamics to enable mobile robots in field environments to efficiently estimate their dynamic parameters, including the mass, location of center of gravity, inertia, base compliance and damping. The algorithm uses an onboard robotic arm to generate base motions, which are measured with simple onboard sensors, and fit to a physical model. A mutual information theoretic basis for a metric on parameter identification is developed. This metric provides a measure on how well a given parameter's value is known. Using this metric, the arm trajectory is defined. Simulations and experimental results show the effectiveness of this algorithm.

8. REFERENCES

- Alloum, A.; Charara, A.; Machkour, H. *Parameters nonlinear identification for vehicle's model*. Proceedings of the 1997 IEEE International Conference on Control Applications. 5-7 Oct. 1997. Hartford, CT, USA.
- Armstrong, B. *On finding exciting trajectories for identification experiments involving systems with nonlinear dynamics*. International Journal of Robotics Research, Vol. 8, No. 6, December 1989.
- Atkeson, C.G., An, C.H., and Hollerbach, J.M. *Estimation of inertial parameters of manipulator loads and links*. Int. Jour. of Robotics Research. Vol. V, No. 3, 1986.
- Bard, Y. *Nonlinear parameter estimation*. Academic Press. London, 1974.
- Baumgartner, E.T., P. S. Schenker, C. Leger, and T. L. Huntsberger. *Sensor-fused navigation and manipulation from a planetary rover*. Proc. SPIE Symp. on Sensor Fusion and Decentralized Control in Robotic Sys., Boston, MA, Nov 1998.
- Gautier, M. and Khalil, W. *Exciting trajectories for the identification of base inertial parameters of robots*. International Journal of Robotics Research, Vol. II, No. 4, August 1992.
- Gelb, A. *Applied optimal estimation*. 1974, MIT press,

Cambridge, MA, U.S.A.

Halfmann, C., Nelles, O. and Holzmann, H. *Modeling and identification of the vehicle suspension characteristics using local linear model trees*. Proc. of 1999 IEEE Int. Conf. on Control Applications, Hawaii, USA, August 22-27, 1999.

Harris, C.J.; Wu, Z.Q.; Gan, Q. *Neurofuzzy state estimators and their applications*. 1999 IEE Colloquium on Advances in Control Technology. 25 May 1999, London, UK.

Hootsman, N.A.M., Dubowsky, S. and Mo, P.Z. *The experimental performance of a mobile manipulator control algorithm*. Proc. of the 1992 IEEE ICRA, Nice, France, May 10-15, 1992. Vol. 3, pp. 1948-1954.

Huntsberger, T.L. *Autonomous multi-rover system for complex planetary retrieval operations*. Proc. SPIE Symp. on Sensor Fusion and Decentralized Control in Autonomous Robotic Agents, Pittsburgh, PA, Oct 1997, pp. 220-229.

Ljung, L and Glad, T. *Testing global identifiability for arbitrary model parameterizations*. Identification and System Parameter Estimation, Vols 1,2. Pergamon Press, New York 1991, pp. 10877-1082.

Majjad, R. *Estimation of suspension parameters*. Proceedings the 1997 IEEE International Conference on Control Applications. 5-7 Oct. 1997, Hartford, CT, USA.

Mayeda, H., Yoshida, K. and Osuka, K. *Base parameters of manipulator dynamics*. Proc. of IEEE Int. Conf. on Robotics and Automation. April 24-29, 1988. Philadelphia, U.S.A.

Nelles, O. and Isermann, R. *Basis function networks for interpolation of local linear models*. Proc. of IEEE Conference on Decision and Control. Kobe, Japan, 11-13 December 1996.

Nikraves, P.E. *Computer-aided analysis of mechanical systems*. Prentice Hall, Englewood Cliffs, NJ, 1988

Olsen, H.B. and Beckey, G.A. *Identification of parameters in models of robots with rotary joints*. Proc. of IEEE Int. Conf. on Robotics and Automation, St. Louis, March 25-28, 1985.

Osborn, J.F. *Applications of Robotics in Hazardous Waste Management* Proceedings of the SME 1989 World Conference on Robotics Research, Gaithersburg, MD.

Schmidt, T. and Muller, P.C. *A parameter estimation method for multibody systems with constraints*. Advanced Multibody System Dynamics: Simulation and Software Tools. Kluwer Academic Publishers, 1993, pp 427-432.

Serban, R. and Freeman, J.S. *Identification and identifiability of unknown parameters in multibody dynamic systems*. Multibody Systems Dynamics. Vol. 5, No. 4, pp. 335-350, May 2001. Kluwer Academic Publishers.

Shaffer, G.; Stentz, A. *A robotic system for underground coal mining*. Proc. of 1992 IEEE ICRA. Page: 633 -638 vol.1

Shannon, C. E. *A mathematical theory of communication*. The Bell System Technical Journal, vol. 27, pp. 379-423 and 623-656, July and October, 1948.

Soderstrom, T and Stocia, P. *System identification*. Prentice Hall International. London, 1989.